Polymer Bulletin 53, 43–52 (2004)
DOI 10.1007/s00289-004-0307-8

Polymer Bulletin

The Dynamics of Solvent Evaporation from Hydroxypropylcellulose/Methanol Solutions with Lyotropic Liquid Crystalline Capability

Carl Lawrence Aronson[1](✉) , John C. Catalogna[1] and William D. Webster[2]

[1]Department of Science and Mathematics and [2]Department of Mechanical Engineering, Kettering University, 1700 West Third Avenue, Flint, Michigan 48504 USA

E-mail: caronson@kettering.edu; Fax: (810) 762-7979

Received: 8 September 2004 / Revised version: 22 October 2004 / Accepted: 22 October 2004
Published online: 8 November 2004 –

Summary

Thin films of hydroxypropylcellulose (HPC)/methanol (MeOH) solutions were juxtaposed against air in a diffusion couple geometry at room temperature and the solvent was allowed to diffuse away and evaporate from the solution in a controlled manner. The diffusion couple geometry produced a uniform film for optical assessment of liquid crystalline potential between crossed polarizers. After an induction period, a stable microstructure developed in which the interior of the sample remained isotropic followed by a cholesteric liquid crystalline band, with characteristic disclination defects and texture, followed by a crystalline band nearest to the external surface. The width of the total characteristic birefringent band was measured over time and provided information concerning the dynamics and trajectory of solvent transport and evaporation from the cover slip edge. The apparent solvent diffusion coefficient for the HPC/MeOH system was measured at room temperature as a function of initial concentration. Diffusion couple optical microscopy data were compared to both solution rheological characteristics as well as model diffusion data from finite difference calculations in order to validate the observed concentration dependence of diffusion.

Introduction

An important area of polymer physics research at the present time is the observation and prediction of *lyotropic* liquid crystalline phase behavior. Lyotropic liquid crystallinity specifically refers to molecular ordering in one or two dimensions (*i.e.* orientational and/or positional) and concomitant phase separation due solely to variations in polymer concentration at constant temperature [1-2]. Lyotropic liquid crystals occur ubiquitously in living systems [3-4]. However, both natural and synthetic lyotropic polymer systems are conventionally composed of a mesogenic polymer and a low molecular weight, *non*-mesogenic solvent. Many different types of macromolecular structures have been shown to exhibit lyotropic behavior, including polymeric amphiphiles (surfactants), rigid main-chain (backbone) polymers as well as flexible segment block copolymers when dissolved in selective solvents [5].

For rigid chain polymers, which would not otherwise demonstrate a *meso*phase, an important consequence of solvent addition is that liquid crystallinity can be attained at temperatures far below their degradation point. Hence, lyotropic capability has become a convenient route to lower a polymer's processing temperature while taking advantage of its rheological characteristics in the liquid crystalline state. As the polymer concentration is increased beyond the lyotropic onset, a biphasic solution is microscopically observed due to molecular ordering (*i.e.* order parameter, S>0). With further increases in concentration, the viscosity of the solution begins to monotonically decrease to a minimum within the fully anisotropic part of the phase diagram [6]. For soluble cellulose derivatives, a sharp decrease in viscosity is normally measured within the concentration region where the anisotropic phase is first microscopically observed [7-8]. This rheological behavior is opposite to solutions containing Gaussian random-coil polymers where sharp increases in viscosity are conventionally measured as a function of increasing polymer concentration. An additional advantage for concentrated lyotropic polymer solutions is the significantly smaller amount of solvent wasted for systems requiring wet-processing.

In the experiments here, mass transport of the solvent is measured for a polymer system possessing lyotropic capability. In addition to its role in the establishment of the lyotropic mesophase, the solvent's evaporative diffusion coefficient is a key parameter in an assortment of design processes that govern the utility and manufacture of a variety of commercial products. These applications include the controlled release of microencapsulated drugs and pesticides, drying of paints, coatings and surfactants; dyeing of fabrics, membrane separation processes, packaging barrier membranes as well as the devolatilization unit operation *post*-polymerization. Calculation of the solvent's diffusion coefficient is also necessary for optimizing the degree of orientation and minimizing processing time in the production of electrically oriented polymer network thin films from lyotropic solutions for optical applications [9].

For many years metallurgists have used the diffusion couple geometry, in which two different substances are juxtaposed, to determine the *inter*-diffusion coefficient of binary metal systems. We aim to demonstrate the applicability of the diffusion couple geometry for quantitatively determining the diffusion and evaporation rate of solvent away from polymer solutions possessing lyotropic liquid crystalline capability. In the diffusion couple geometry the polymer solution is juxtaposed against air and the solvent is allowed to diffuse away and evaporate from the solution in a controlled manner as shown in Figure 1.

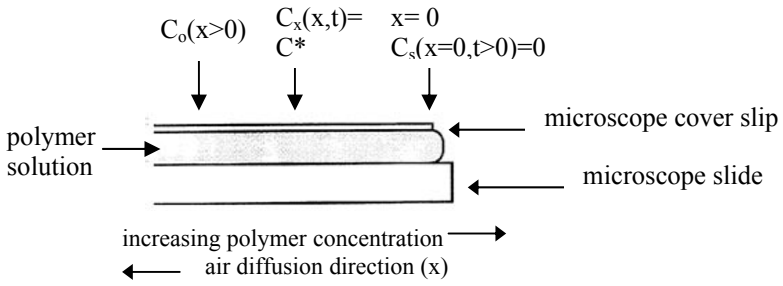

Figure 1. Schematic side-view of the liquid crystalline diffusion couple geometry with indicated *solvent* concentration (C), air diffusion direction (x) as well as proposed initial solvent concentration (C_o), lyotropic phase transition (C*) and air interface boundary (C_s) condition

A number of cellulose derivatives have been noted to possess lyotropic liquid crystalline potential [10-14]. Hydroxypropylcellulose (HPC) specifically forms an ordered liquid crystalline phase with cholesteric structure when concentrated in either aqueous solution [15-28] or polar organic solvents such as methanol or ethanol [5, 29-31]. HPC is commercially available in a range of molecular weights and consists of a highly substituted cellulose ether prepared by the base catalyzed reaction of propylene oxide with cellulose at elevated temperatures and pressures [32-34]. The propylene oxide can potentially be substituted on the cellulose through an ether linkage at each of the three reactive hydroxyl groups present on each anhydroglucose monomer unit within the cellulose chain [35]. Nevertheless, etherification has been observed to produce hydroxypropyl substituents containing almost exclusively secondary hydroxyl groups [36-37]. In addition, propylene oxide may react with secondary hydroxyl groups on previously attached hydroxypropyl substituents causing side-chain formation. An idealized repeat structure for the HPC molecule is shown in Figure 2 below.

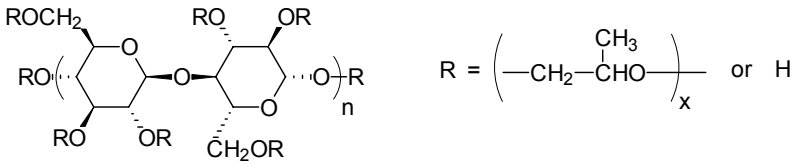

Figure 2. Idealized chemical repeat structure of hydroxypropyl cellulose with a number of hydroxypropyl groups *per* anhydroglucose residue

In addition, the chain diameter (d) for HPC has been measured to lie between 8.1 and 10.4 angstroms with a typical persistence length (q) of 70-100 angstroms (*i.e.* axial ratio of the Kuhn segment ($2q/d$) =13.5-19.2) [5]. Hence, the HPC chain character has been modeled as a freely jointed rod/*Kuhn* chain at relatively high molecular weights (*i.e.* high polymer chain length, $L>>2q$). The rheology of HPC aqueous or polar organic solutions as a function of increasing polymer concentration was observed to follow conventional behavior for polymer systems possessing lyotropic potential: a monotonic increase in viscosity below the lyotrope followed by a monotonic decrease in viscosity beginning near the lyotropic liquid crystalline onset [7-8].

For HPC/MeOH solutions, the diffusion couple geometry shown in Figure 1 produces a thin, uniform film for optical microscopic assessment of liquid crystalline potential between crossed polarizers. In this geometry, diffusion is a direct consequence of the gradient in chemical potential produced by solvent evaporation as well as the negative enthalpy of solvation for the lyotropic polymer. Hence, evaporative techniques using the diffusion couple geometry were primarily investigated here in order to develop a potentially facile method to extract critical quantitative and qualitative information concerning polymer-solvent thermodynamic interactions. In addition, the diffusion couple technique appears to uniquely allow simultaneous microscopic examination of the dynamics of solvent diffusion and evaporation as well as subsequent microstructural changes during drying of polymer solutions possessing lyotropic capability.

Experimental

Materials

HPLC grade methanol (MeOH) and hydroxypropyl cellulose (HPC) were obtained from the Aldrich Chemical Company (Milwaukee, WI) and used as received. The nominal value for HPC weight average molecular weight (M_w) was 100,000 g/mole [32-34].

Solution Preparation

Polymer samples were prepared by adding a weighed amount of solvent to a weighed amount of dried polymer. Precautions were taken to minimize losses due to solvent evaporation using capped and sealed vials. A period of several days was allowed between HPC/MeOH solution sample preparation and optical assessment in order to ensure complete dissolution.

Polarized Optical Microscopy

All polarized optical microscopy (POM) was performed at room temperature (T=23°C) on a Nikon® cross polarizing microscope with an objective lens magnification of 10-40x and an Olympus® microscope eyepiece (WF10XMicro, Tokyo, Japan) with a magnification of 10 times using transmitted polarized light. Length scales were calibrated using 100 gradations in the Olympus® microscope eyepiece (WF10XMicro, Tokyo, Japan) along with a 0.01 mm objective micrometer (Nikken Company, Tokyo, Japan).

Diffusion Couple Experiments

A small amount of polymer solution of known concentration was initially confined between a microscope glass slide (borosilicate, 3 inch x 1 inch x 1 mm thick, Fisher Scientific, Pittsburgh, PA) and a 18 mm square glass cover slip (Corning Glass Company, Corning, NY) in the polarized optical microscope (Figure 1). Only a few drops of solution were used to form a thin (~5-10 micrometers thick) film covering the entire area beneath the cover slip, lying almost exclusively underneath and not outside the edge of the cover slip as illustrated in Figure 1. The thin film specimens were placed between crossed polarizers and analyzed at consistent time intervals over several hours as the methanol solvent diffused and evaporated from the solution. Initial polymer concentrations ranged from the *semi*-dilute to the concentrated region below the lyotropic transition.

Results and Discussion

The concentration of polymer required to form an ordered phase was found by assessing and bracketing a series of HPC/MeOH solutions of known concentration using cross-polarized optical microscopy techniques. The minimum HPC concentration required for *meso*phase formation was found to be approximately 43% (wt/wt) or 37% (vol/vol) assuming additivity of component volumes (ρ_{HPC} = 1.20 g/ml and ρ_{MeOH} = 0.79 g/ml) in close agreement with Werbowyj and Gray [29]. After a

relatively short period of time (≤ 1-2 minutes), a stable microstructure developed in which the interior of each solution remained isotropic. The isotropic region was followed by a liquid crystalline band, with nucleation and growth regions as well as characteristic disclination defects and cholesteric *Schlieren* texture [38], followed by a virtually solid crystalline band (resistant to shear deformation) nearest to the external surface. In the liquid crystalline phase, a supramolecular helicoidal arrangement of HPC rods in a cholesteric phase of pitch, P (*z*-direction), where the microscope glass, cover slip, and long axis of the aligned polymer chains were all in the *xy* plane was assumed [18]. The width of each particular characteristic birefringent band was observed to grow with time and measurement of a band's width provided information about the dynamics of solvent transport and evaporation from the cover slip edge. The data collected here consisted of the *sum* width (x) of the birefringent crystalline *and* lyotropic liquid crystalline phases over time (t) at a fixed temperature (T) and initial *solvent* concentration (C_o) as shown in Figure 3.

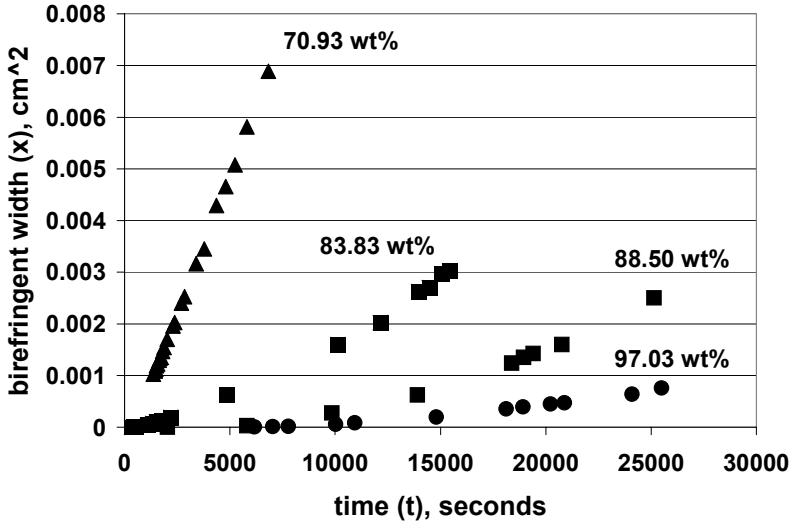

Figure 3. Representative birefringent band width (x, cm^2) measurements versus time (t, seconds) denoted as a function of initial MeOH solvent concentrations (C_o, % (wt/wt)) with HPC (M_w = 100,000 g/mole) at T=23°C

The lyotropic onset *solvent* concentration, $C_x(t)$, observed in the diffusion couple was assumed to correspond to the static, microscopically measured liquid crystalline phase diagram for methanol with HPC (C*=57 wt%) [29]. Hence, the lyotropic onset (C*) was assumed to be independent of initial solvent concentration (C_o) during diffusion dynamics. The kinetics of the mesophase transition at C* were assumed to be fast compared to the solvent diffusion rate. In addition, complete drying at the cover slip edge (x=0) was assumed to occur quickly compared to the establishment of steady-state diffusion (*i.e.* $C(x=0) = C_s \cong 0$ at time (t) > 0) and the edge concentration was assumed to be independent of initial solvent concentration ($C_s \neq f(C_o)$). A simple *iso*-thermal Fickian model (equation 1), which assumes that diffusion distance squared (x^2) is proportional to time (t), as well as *semi*-infinite boundary conditions (equations

(2)-(4)) were initially applied to the experimental birefringence data in order to calculate the solvent's *apparent* diffusion coefficient ($D^{apparent}$).

$$\partial C/\partial t = D^{apparent} (\partial^2 C/\partial x^2) \quad (\mathbf{1})$$

$$C(x = 0, t > 0) = C_s = 0 \quad (\mathbf{2})$$

$$C(x > 0, t = 0) = C_o \quad (\mathbf{3})$$

$$C_x(x,t) = C^* \text{ (lyotropic onset).} \quad (\mathbf{4})$$

With the assumptions detailed above, the solution to the partial differential diffusion equation (1) became:

$$(C_o - C_x)/(C_s - C_o) = \text{erfc}(x / (4 D^{apparent} t)^{½}) \quad (\mathbf{5})$$

and since $C_s = 0$ at $t > 0$ from the boundary condition (equation 2),

$$C_x / C_o = \text{erf}(x/ \sqrt{4 D^{apparent} t}) \quad (\mathbf{6})$$

which upon rearrangement becomes

$$x^2 = 4 D^{apparent} t [\text{inverf} (C_x/C_o)]^2 \quad (\mathbf{7})$$

or

$$D^{apparent} = (\text{slope of } x^2\text{-}t \text{ plot}) / 4 [\text{inverf} (C_x/C_o)]^2. \quad (\mathbf{8})$$

Application of *semi*-infinite boundary conditions here appeared reasonable due to the final experimental penetration depth being ≤ 0.1% of the total distance (½ of the square microscope cover slip dimension in one direction). Preliminary results from the HPC (M_w = 100 kg/mole)/MeOH system indicated Fickian diffusion (*i.e.* x^2 varies linearly with t) behavior for each independent initial solution concentration (C_o) as shown in Figure 3. The apparent diffusion coefficient ($D^{apparent}$), calculated using equation (8), was plotted as a function of initial MeOH solvent concentration (C_o) in Figure 4. Throughout the Fickian model (equations (1)-(8)), $D^{apparent}$ was assumed to be independent of initial *solvent* concentration (C_o) for $C_s < C < C_x$. Nevertheless, opposite to the Fickian model, the diffusion coefficient was observed to be highly concentration dependent and polynomial (quadratic) in C_o for the HPC/MeOH system as illustrated in Figure 4.

Intriguingly, concentration dependent diffusion was observed for other lyotropic polymer systems including poly(*n*-hexyl isocyanate) (PHIC)/xylene. PHIC is a member of the 1-nylon class and is an archetypical helicoidal, semiflexible-persistent chain that is uniquely highly soluble in *non*-polar organic solvents despite its relatively large dipole moment [5]. PHIC forms a lyotropic *nematic* phase in xylene [39]. Nevertheless, the PHIC/xylene system was observed to follow similar polynomial concentration dependence for diffusion compared to the lyotropic cholesteric HPC/MeOH system (Figure 4). This similarity lends credence to the plausible universal applicability of the diffusion couple technique for lyotropic polymer systems.

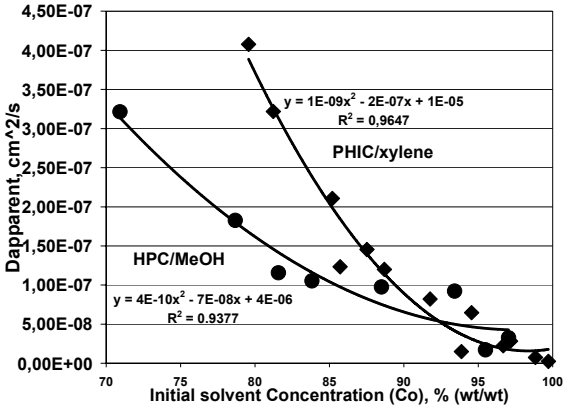

Figure 4. Apparent diffusion coefficient ($D^{apparent}$, cm^2/s) versus initial solvent concentration (C_o, wt%) at T=23°C for HPC/MeOH and poly(*n*-hexyl isocyanate) (PHIC, C*=73% (wt/wt), M_w=129 kg/mole; PDI = 2.34)/xylene [39]

Several different mathematical techniques were employed to model the concentration dependence of the HPC/MeOH diffusion coefficient. Nevertheless, attempts to normalize the concentration dependence were initially unsuccessful. Furthermore, a fundamental model for the concentration dependence of the solvent's diffusion coefficient in lyotropic polymer systems has not been presented in the literature to date to the best of our knowledge. A numerical computer code was written employing Crank-Nicholson predictor-corrector one-dimensional finite differences mathematical techniques to solve the partial differential diffusion equation (1) given $D^{apparent}(C_o)$, initial condition {$C(x,t=0) = C_o$} and assuming either *semi*-infinite {$C(x=0,t) = 0$ and $C(4,t) = C_o$} or symmetrical-source {$C(x=0,t) = 0$ and $MC/Mx\ (W/2,t) = 0$} boundary conditions, where 2W is the length of the entire microscope glass cover slip. Diffusion profiles for concentration, % (wt/wt) versus normalized diffusion length scale over time (t) were generated using the quadratic regression analysis for HPC/MeOH shown in Figure 4 (*i.e.* $D^{apparent}(C_o) = 4x10^{-10}\ x^2 - 7x10^{-8}\ x + 4x10^{-6}$). The theoretical diffusion profile for HPC/MeOH at C_o = 85% (wt/wt), using step sizes of Δt =100 seconds and Δx = 1% of the total normalized diffusion length scale is shown in Figure 5.

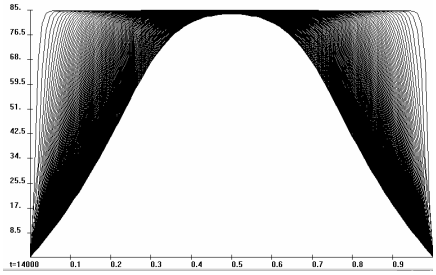

Figure 5. Symmetric diffusion profile for HPC/MeOH system over the entire diffusion couple calculated using Crank-Nicholson predictor-corrector one-dimensional finite differences mathematical techniques over t = 14000 seconds, where $D^{apparent}(C_o) = 4x10^{-10}\ x^2 - 7x10^{-8}\ x + 4x10^{-6}$, C_o = 85% (wt/wt) and step sizes Δt =100 seconds and Δx = 1% of the total normalized length

Calculated (x,t) data pairs were compared to the experimental diffusion couple data in order to validate the concentration (C_o) dependence of the experimentally determined apparent diffusion coefficient ($D^{apparent}$). In general, the trend for the calculated (x,t) data were in good agreement with the actual (x,t) diffusion data *sans* an initial induction time period required to experimentally establish steady-state diffusion. Deviation between experimental diffusion data and theoretical calculations were ascribed primarily to the imperfect quadratic fit of $D^{apparent}$ as a function of C_o for the HPC/MeOH system as illustrated in Figure 4. Nevertheless, although higher order polynomial regression fits for $D^{apparent}(C_o)$ provided a lower standard deviation, periodic instability using the present Crank-Nicholson computer code was noted. Hence, further refinement of the finite differences model code is needed.

$D^{apparent}$ was observed to decrease monotonically with increasing C_o for initial solvent concentration above the lyotropic onset (C_o>C*) in Figure 4. Hence, starting at a solution concentration closer to the lyotropic transition effectively caused faster solvent diffusion in the HPC/MeOH system. The viscosity of cellulose derivative solutions possessing lyotropic cholesteric capability show a monotonic increase in diffusion at solvent concentrations above C* and a monotonic decrease at solvent concentrations below C* [7-8.] We hypothesize that the morphology and concomitant rheology of the HPC/methanol system play a large role in effectively dictating the diffusion rate of MeOH through the HPC matrix. At a solvent concentration below C*, the polymer chains begin to macroscopically align (S>0), thereby significantly decreasing the overall resistance and tortuosity for methanol solvent flow. Methanol molecules were apparently able to diffuse through the organized, lyotropic mesophase at a significantly enhanced rate compared to the amorphous phase. Furthermore, cross-polarized examination of the lyotropic domains, and more specifically the dried crystalline region nearest to the cover slip edge, *via* rotation of the microscope stage, revealed extinction characteristics consistent with orientation. Hence, solvent diffusion and evaporation apparently produced a field similar to a small shear stress and the methanol diffusional path was proposed to be primarily dictated by polymer chains within aligned liquid crystalline domains. Oppositely, at solvent concentrations above C*, the polymer chains were not macroscopically aligned (S≅0) and evaporative diffusion merely increased the resistance for solvent flow. In the HPC/MeOH system, starting closer to the lyotropic onset appeared to significantly enhance the diffusion rate. Hence, it is hypothesized here that solvent transport in the diffusion couple geometry was viscosity controlled. Furthermore, two opposing regimes existed on either side of the lyotropic onset and the effect of organization at the *lyotropic* cholesteric transition was effectively dominant in the HPC/MeOH system.

Conclusions

Measurement of HPC/MeOH solutions with known initial concentration using the diffusion couple geometry produced an *apparent* Fickian diffusion coefficient. Nevertheless, opposite to the Fickian model the apparent diffusion coefficient was observed to be concentration dependent but follow rheological trends. The apparent Fickian diffusion coefficient garnered from the diffusion couple geometry can be utilized to optimize the degree of orientation and minimize processing time for oriented polymer thin films. The concentration dependence of the apparent diffusion coefficient for lyotropic-nematic poly(*n*-hexyl isocyanate)/xylene solutions was

observed to follow similar polynomial concentration dependence as the lyotropic cholesteric HPC/MeOH system. Hence, the HPC/MeOH system encompasses the initial part of a study aimed at establishing a *chemical structure-morphology-diffusion rate* relationship among lyotropic polymer classes. Several lyotropic polymer systems with different polymer chain stiffness/persistence lengths (*i.e.* rigid-rod, freely jointed rod, semiflexible-persistent chain, coil-coil diblock chain) and liquid crystalline morphologies (*i.e.* nematic, cholesteric, smectic) are under investigation as a function of temperature and initial concentration. The dependence of the solvent's diffusion coefficient on concentration and temperature will be examined individually for each system. The concentration dependence and activation energy trends for diffusion will then be compared in order to evaluate the universal applicability of the diffusion couple quantitative method for evaluating the solvent's diffusion rate in lyotropic polymer systems.

References

1. Donald AM, Windle AH (1993) Liquid Crystalline Polymers. Cambridge University Press, UK
2. DeGennes PG, Prost J (1993) The Physics of Liquid Crystals. 2nd Edition, Clarendon Press, Oxford, UK, pp 6 (1993)
3. Chandrasekhar S, Liquid Crystals.(1992) 2nd Edition, Cambridge University Press, UK, pp 12-14
4. Chapman D, (1971) Faraday Soc Symp 5:165
5. Ciferri A (1991) "Phase Behavior of Rigid and Semirigid Mesogens." In: Liquid Crystallinity in Polymers. VCH Publishers, New York, Chapter 4, pp 209-259
6. Aharoni SM (1980) Polymer 21:1413
7. Aharoni SM (1981) J Polym Sci, Polym Lett Ed 19:495
8. Dayan S, Maissa P, Vellutini MJ, Sixou P (1982) J Polym Sci, Polym Lett Ed, 20:33
9. Martin DC (2002) Polymer 43:4421
10. Gray DW, J (1983) Appl Polym Sci, Appl Polym Symp 37:179
11. Tseng SL, Valente A, Gray DW (1981) Macromoleules 14:715
12. Dayan S, Fried F, Gilli JM, Sixou P (1983) J Appl Polym Sci, Appl Polym Symp 37:193
13. Zugenmaier P, J Appl Polym Sci, Appl Polym Symp, 37:223
14. Navard P, Haudin JM, Dayan S, Sixou P (1981) J Polym Sci, Polym Lett Ed 19:379
15. Werbowyj RS, Gray DG (1976) Mol Cryst Liq Cryst Lett, 34:97
16. Maeno J, (1979) US Patent 4,132,464
17. Chiba, R, Nishio Y (2003) Macromolecules 36(5):1706
18. Gray DG (1983) J Appl Polym Sci, Appl Polym Symp 37:179
19. Gilbert RD, Patton PA, (1983) Prog Polym Sci 9:115
20. Gray DG Faraday Discuss Chem Soc (1985) 79:257
21. Guo JX, Gray DG (1994) In: . Gilbert RD (ed) Cellulosic Polymers, Blends and Composites. Carl Hanser, Munich, Chapter 2
22. Fortin S, Charlet G (1989) Macromolecules 22:2286.
23. Godinho MH, Fonseca JG, Ribeiro AC, Melo LV, Brogueira P. (2002) Macromolecules 35(15):5932
24. Navard P, Haudin JM, Dayan S, Sixou, P (1983) J Appl Polym Sci, Appl Polym Symp 37:211
25. Aspler JS, Gray DG (1979) Macromolecules 12:562
26. Aspler JS, Gray DG (1981) Macromolecules 14:1546
27. Onogi Y, White JL, Fellers JF (1980) J Polym Sci, Polym Phys Ed 18:663
28. Onogi Y, White JL, Fellers JF (1980) J Non-Newtonian Fluid Mech, 7:121
29. Werbowyj RS, Gray DG (1980) Macromolecules, 13:69
30. Tsutsui T, Tanaka R (1980) Polym J 12:473

31. Aharoni SM, (1981) Am Chem Soc Polym Prep 22(1):116
32. Standard Test Methods for Hydroxypropylcellulose (2003) Test D 5400-03 American Society for Testing and Materials (ASTM), West Conshohocken, Pennsylvania
33. Klug ED, (1971) J Polym Sci, Polym Symp 36:49
34. Klug ED, "Hydroxypropylcellulose" (1971) In: Bikales NM (ed) Encyclopedia of Polymer Science and Technology. Volume 15, Wiley-Interscience, New York, pp 307-314
35. Standard Test Method for Methoxyl and Hydroxypropyl Substitution in Cellulose Ether Products by Gas Chromatography (2001) Test D 3876-96 American Society for Testing and Materials (ASTM), West Conshohocken, Pennsylvania
36. Hydroxypropyl Cellulose: Physical and Chemical Properties. (2001) Hercules Inc (Aqualon), Wilmington, Deleware, p 4
37. Savage AB Derivatives of Cellulose: Ethers.(1971) In: Bikales, NM, Segal L (ed) In: Cellulose and Cellulose Derivatives Part V, 2nd Edition, High Polymers (Part V), Wiley-Interscience, New York, Chapter 17c, pp 806-807
38. Shimamura K, White JL, Fellers JF (1981) J Appl Polym Sci 26:2165
39. Aronson, CL (2000) "Structure-Property Relationships for *n*-Alkyl Isocyanate Containing Polymers." Ph.D. Dissertation University of Michigan, Ann Arbor